

Moment analysis of the probability distribution of different sandpile models

S. Lübeck*

Theoretische Tieftemperaturphysik, Gerhard-Mercator-Universität Duisburg, Lotharstrasse 1, 47048 Duisburg, Germany

(Received 1 April 1999)

We reconsider the moment analysis of the Bak-Tang-Wiesenfeld and the stochastic sandpile model introduced by Manna [J. Phys. A **24**, L363 (1991)] in two and three dimensions. In contrast to recently performed investigations our analysis reveals that the models are characterized by different scaling behavior, i.e., they belong to different universality classes.

PACS number(s): 64.60.Ht, 05.65.+b, 05.40.-a

I. INTRODUCTION

The Bak-Tang-Wiesenfeld (BTW) model was introduced as a paradigm of the concept of self-organized criticality which describes the emergence of spatiotemporal correlations in slowly driven dissipative systems [1,2]. Despite its analytical tractability [3] the scaling behavior of the two-dimensional BTW model is not well understood. Especially the exponents which determines the avalanche distributions are not known exactly. Several numerical attempts were made but do not provide consisting results [4–10]. Recently De Menechet *et al.* performed a moment analysis of the BTW model [11] which was extended by several authors to different sandpile models [12–14]. Especially the moment analysis of the size distribution of the BTW and Manna sandpile model has led Chessa *et al.* to the conclusion that both models are characterized by the same scaling exponents and thus belong to the same universality class [12]. In this work we reconsider the moment analysis and compare the scaling behavior of various avalanche quantities for the BTW and Manna model. Our analysis turns out that in contrast to [12] the moment behavior of both models differs significantly, i.e., the BTW and the Manna model belong to different universality classes.

II. MODELS AND SIMULATIONS

The BTW model is defined on a D -dimensional square lattice of linear size L in which non-negative integer variables $E_{\mathbf{r}}$ represent a physical quantity such as the local energy, stress, height of a sand column, etc. One perturbs the system by adding particles at a randomly chosen site \mathbf{r} according to

$$E_{\mathbf{r}} \rightarrow E_{\mathbf{r}} + 1, \quad \text{with random } \mathbf{r}. \quad (1)$$

A site is called unstable if the corresponding variable exceeds a critical value E_c , i.e., if $E_{\mathbf{r}} \geq E_c$, where the critical value is given by $E_c = 2D$. An unstable site relaxes, its value is decreased by E_c and the two-dimensional (2D) nearest neighboring sites are increased by one unit, i.e.,

$$E_{\mathbf{r}} \rightarrow E_{\mathbf{r}} - E_c, \quad (2)$$

$$E_{nn,\mathbf{r}} \rightarrow E_{nn,\mathbf{r}} + 1. \quad (3)$$

In this way the neighboring sites may be activated and an avalanche of relaxation events may take place. These avalanches are characterized by several physical properties like the size s (number of relaxation events), the area a (number of distinct toppled sites), the time t (number of parallel updates until the configuration is stable), the radius r (radius of gyration), the perimeter p (number of boundary sites), etc. In the critical steady state the corresponding probability distributions should obey power-law behavior [1]

$$P_x(x) \sim x^{-\tau_x} \quad (4)$$

characterized by the avalanche exponents τ_x with $x \in \{s, a, t, r, p\}$. Assuming that the size, area, etc. scale as power of each other,

$$x \sim x'^{\gamma_{xx'}}, \quad (5)$$

one obtains the scaling relations $\gamma_{xx'} = (\tau_{x'} - 1) / (\tau_x - 1)$. The scaling exponents $\gamma_{xx'}$ describe the static avalanche properties as well as its propagation. For instance, the exponent γ_{sa} indicates if multiple toppling events are relevant ($\gamma_{sa} > 1$) or irrelevant ($\gamma_{sa} = 1$). The exponent γ_{ar} equals the fractal dimension of the avalanches. A possible fractal behavior of the avalanche boundary corresponds to the inequality $D - 1 < \gamma_{pr} < D$. Finally, the exponent γ_{tr} is usually identified with the dynamical exponent z .

A stochastic version of the BTW model was introduced by Manna [15]. Here, critical sites relax to zero, i.e., $E_{\mathbf{r}} \rightarrow 0$ if $E_{\mathbf{r}} \geq E_c$ and the removed energy is randomly distributed to the nearest neighbors in the way that one chooses randomly for each energy unit one neighbor. For $E_c = 1$ the behavior of the model corresponds to a simple random walk. Above this value ($E_c \geq 2$) is the choice of the critical energy irrelevant to the scaling behavior (see Fig. 1).

Recently Dhar introduced a modified version of the two-dimensional Manna model where the energy of critical sites is not reduced to zero but $E_{i,j} \rightarrow E_{i,j} - 2$. The energy $\Delta E = 2$ is then equally distributed with probability 1/2 to the sites $(i \pm 1, j)$ or otherwise to the sites $(i, j \pm 1)$ [16]. In this case it is possible to extend an operator algebra, which was successfully applied in studying the BTW model [3], to this modified Manna model.

Compared to the BTW model the dynamics of the Manna model with its stochastic distribution of the energy to the nearest neighbors can be interpreted as a disorder effect. A different kind of disorder effects were investigated in di-

*Electronic address: sven@thp.uni-duisburg.de

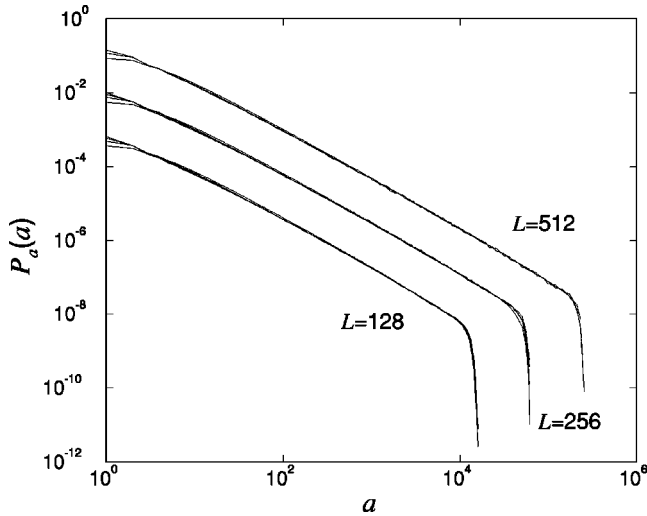


FIG. 1. The probability distribution $P_a(a)$ of the two-dimensional Manna model for $E_c \in \{2,3,5,10\}$ and various system sizes L . For $L < 512$ the curves are shifted in the downward direction. No significant difference between the curves for different values of the critical energy can be observed, i.e., E_c does not affect the scaling behavior of the model.

rected sandpile models by introducing stochastic toppling conditions. In particular the exact solution of the directed BTW model [17] was used as a starting-point in order to examine how the known scaling behavior of the system is affected by the stochastic toppling rules. Depending on the details of the introduced disorder a collapse of the critical behavior [18], nonuniversal critical behavior [19,20] as well as a crossover to the different universality class of directed percolation [21] was observed.

Thus an important question is if the scaling behavior of the Manna model differs from the scaling behavior of the BTW model, i.e., if the additional fluctuations of the Manna model could change the universality class. A real-space renormalization scheme predicted that both models belong to the same universality class [22,23]. Here, the authors used a mean-field-type approximation [24] in order to perform a block transformation. Therefore it is not clear if this renormalization ansatz is an appropriate tool to take the additional fluctuations of the energy distribution of the Manna model into account.

A momentum space analysis of Langevin equations of the BTW and the related Zhang model [25] predicted that both models are characterized by the same exponents [26,27] and numerical investigations confirmed this prediction [8,28]. Unfortunately up to now no extension of the momentum space analysis to the Manna model could be performed. The crucial point of this renormalization approach is the choice of an appropriate noise correlator [27]. Compared to the BTW model the corresponding analysis of the Manna model requires a different noise correlator. But a different noise-correlators could lead to a different critical behavior (see for instance [29]).

The first numerical indication that both models belong to different universality classes was reported by Ben-Hur and Biham [8]. They measured several scaling exponents $\gamma_{xx'}$ via Eq. (5) and found, in particular, that the dynamical exponents z , the multitoppling exponents γ_{sa} and the boundary

exponents γ_{pr} of both models differ significantly. But one has to mention that at least one of the scaling exponents of the BTW model (γ_{sa}) cannot be determined in this way since the assumed scaling behavior $s \sim a^{\gamma_{sa}}$ is not well defined [9,12].

However, the conjecture of Ben-Hur and Biham was confirmed for $D=2$ by a numerical determination of the avalanche exponents τ_s , τ_a , τ_t , and τ_r [9] which again differ significantly for both models. In this analysis the exponents of the Manna model were obtained by a direct regression analysis as well as a simple finite-size scaling analysis of the corresponding probability distributions. In the case of the BTW model it was found that the probability distributions are affected by unconventional logarithmic finite-size corrections [4,9] which lead to uncertain results for the simple finite-size scaling ansatz. Taking these corrections into account it is possible to estimate the values of the exponents [4,9] by an extrapolation to $L \rightarrow \infty$. But one has to note that the assumed logarithmic corrections are found only numerically, i.e., there exist up to now no analytical justification of this unconventional behavior.

These difficulties vanish in the three-dimensional case where both models fulfill the finite-size scaling ansatz which makes the analysis much easier [30]. The accuracy of the determination is sufficient to show that both models belong to different universality classes [30]. Additionally the scaling behavior of the three-dimensional Manna model is strongly affected by multiple toppling events ($\tau_s \neq \tau_a$) whereas it seems that the rare multiple toppling events of the BTW model does not contribute to the scaling behavior [5,30]. Taking this results into consideration we have convincing, but of course not completely rigorous, arguments that the BTW and the Manna model does not belong to the same universality class.

Recently this statement was questioned by Chessa *et al.* [12] who performed a moment analysis of both models in analogy to the investigations of De Menech *et al.* [11]. The q -moment of the probability distribution $P_x(x)$ is defined as

$$\langle x^q \rangle = \int dx x^q P_x(x). \quad (6)$$

The finite system size L causes a cutoff of the probability distribution at $x_{\max} \sim L^{\gamma_{xr}}$. Assuming a power-law behavior of the distributions [Eq. (4)] the scaling behavior of the q -moment is dominated by the upper boundary of Eq. (6)

$$\langle x^q \rangle_L \sim L^{\sigma_x(q)} \quad (7)$$

if $q > \tau_x - 1$ and where the moment exponent $\sigma_x(q)$ is given by

$$\sigma_x(q) = \gamma_{xr}(q + 1 - \tau_x). \quad (8)$$

For $q < \tau_x - 1$ the moment exponent $\sigma_x(q)$ behaves nonlinear with respect to q . The normalization of the probability distributions results in $\sigma_x(q) = 0$ for $q \rightarrow 0$. Performing numerical investigations one can obtain the behavior of the exponent $\sigma_x(q)$ via a regression analysis of $\ln \langle x^q \rangle_L$ as a function of $\ln L$, or via the logarithmic derivative

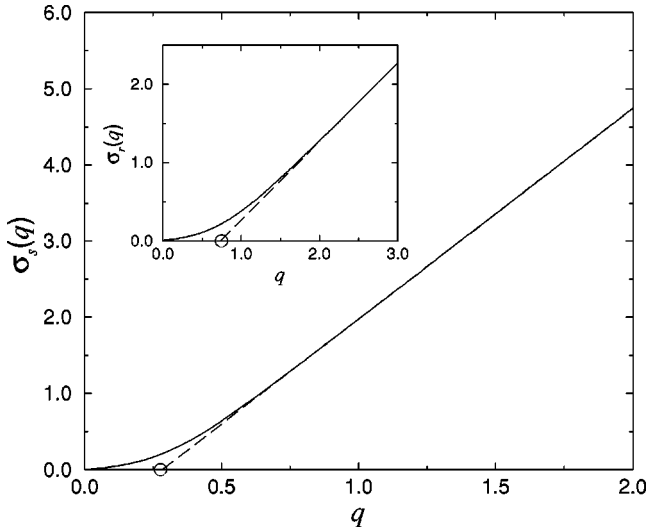


FIG. 2. The exponent $\sigma_s(q)$ and $\sigma_r(q)$ of the two-dimensional Manna model. The extrapolation to the horizontal axis yields the exponents $\tau_s=1.286$ and $\tau_r=1.729$, respectively. The slope corresponds to the scaling exponents γ_{sr} and γ_{rr} where the latter equals one (see Table I). The positions and sizes of the circles on the horizontal axes correspond to the values and error bars of the exponents $\tau_s=1.275\pm 0.011$ and $\tau_r=1.743\pm 0.025$, obtained from a regression analysis [9].

$$\sigma_x(q) = \frac{\partial \ln \langle x^q \rangle_L}{\partial \ln L}. \quad (9)$$

The behavior of $\sigma_x(q)$ as a function of q allows to determine the scaling exponent γ_{xr} , which corresponds to the slope, and the avalanche exponent τ_x which can be obtained from an extrapolation to the horizontal axis [Eq. (8)]. This is shown in Fig. 2 where the exponents $\sigma_s(q)$ and $\sigma_r(q)$ of the Manna model are plotted as a function of q . The values of the exponents are in agreement with those of previous investigations obtained from a regression analysis a finite-size scaling analysis, as well as a moment analysis [9,12]. But one has to mention that the accuracy of the regression analysis is higher than the accuracy of the moment analysis. In the case of the regression analysis one obtains the exponents τ_x by a direct fit to the distribution. Whereas for the moment analysis one has first to calculate the average [Eq. (6)], second to fit the logarithmic derivatives [Eq. (9)] and third to extrapolate to $\sigma_x(q)=0$. This leads to a propagation of errors which increases the uncertainty significantly.

The q -dependence of the moment exponent $\sigma_x(q)$ is determined by the avalanche exponents [Eq. (8)]. Therefore, the moment analysis can be used to distinguish the universality classes of different models. Using the scaling relation $\gamma_{xr}=(\tau_r-1)/(\tau_x-1)$, Eq. (8) now reads

$$\sigma_x(q) = \gamma_{xr}q + \Sigma, \quad (10)$$

with $\Sigma=1-\tau_r$. Thus, we get that the intercept Σ of the linear q -dependence of the moment exponent $\sigma_x(q)$ is the same for all distributions (site, area, duration, etc.) and is therefore a characteristic quantity of the model. Considering two models we get that different values of Σ implies different universality classes. But the same value of the intercept

TABLE I. Exponents γ_{xr} for the BTW and Manna model. The values are obtained from a linear regression according to Eq. (10) and the errors are of the order $\Delta\gamma_{xr}<0.01$. The real error which includes the uncertainty of the whole moment analysis is hard to estimate and increases this value significantly (see text).

	BTW, 2D	Manna, 2D	BTW, 3D	Manna, 3D
γ_{sr}		2.764	3.004	3.302
γ_{ar}	2.021	2.025	3.004	3.076
γ_{tr}		1.540	1.618	1.713
γ_{pr}	1.266	1.42 [8]		
γ_{rr}	1.008	1.006	0.995	1.010

Σ does not imply that both models belong to the same universality class. It is possible that the models display different values of γ_{xr} which results in different values of $\tau_x=1-\Sigma/\gamma_{xr}$. Thus two different models belong to the same universality class if they are characterized by the same linear dependence of $\sigma_x(q)$ for all relevant quantities x .

The determination of the intercept Σ for various distributions allows to estimate the accuracy of the moment analysis. In the case of the Manna model we obtain from the moment analysis of the size, area, duration and radius distribution the values $\Sigma_s=-0.7900\pm 0.002$, $\Sigma_a=-0.7202\pm 0.003$, $\Sigma_t=-0.7684\pm 0.004$, $\Sigma_r=-0.7333\pm 0.005$. The corresponding values of the scaling exponents γ_{xr} are listed in Table I. The above error bars correspond to the uncertainty of the linear regression [Eq. (10)]. The average value $\Sigma_{\text{Manna,2D}}=0.7530\pm 0.037$ agrees with $\Sigma=3/4$ predicted in [9]. The latter error bar reflects the uncertainty of the whole method and could be use as a lower bound for the error of the avalanche exponent $\Delta\tau_r\geq 0.037$. Typical error bars of a direct analysis of the probability distributions are $\Delta\tau_r\leq 0.025$.

III. MOMENT ANALYSIS OF THE BTW AND MANNA MODEL

We now consider the moment analysis of the BTW and Manna model for the size, area, duration, radius, and perimeter distribution and compare the corresponding results. In the case of the BTW model we analyze the probability distributions of lattice sizes up to $L=4096$ for $D=2$ and $L=256$ for $D=3$, respectively. Since the Manna model does not display strong finite-size effects as the BTW model it is sufficient to consider system sizes only up to $L=2048$ for $D=2$.

The moment analysis of the size distribution leded Chessa *et al.* to the conclusion that both models are characterized by the same scaling behavior [12]. Therefore we first consider the size distribution and the corresponding exponent $\sigma_s(q)$ is shown in Fig. 3. In contrast to Chessa *et al.* who found that both models display indistinguishable curves for $q>1$ we get slightly different curves. Plotting the derivative of the exponents $\sigma_s(q)$ with respect to q the differences become more significant (see inset of Fig. 3). In the case of the Manna model the derivative of the exponent saturates quickly with increasing q . Whereas the derivative $\partial_q\sigma_s(q)$ for the BTW model is characterized by a finite curvature, i.e., the exponent γ_{sr} is not well defined in the case of the BTW model. The duration probability distribution displays a simi-

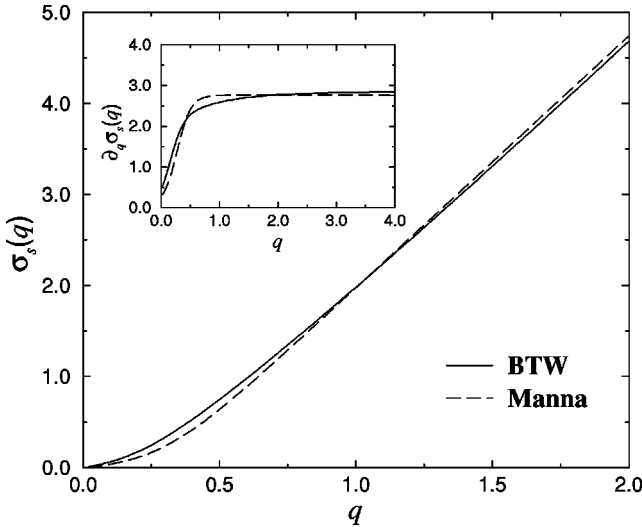


FIG. 3. The exponent $\sigma_s(q)$ of the two-dimensional BTW and Manna model. The curves differ slightly. The derivative of both curves is plotted in the inset and reveals that the exponent $\sigma_s(q)$ of the BTW model is not well defined in the sense that no clear saturation of the exponent can be seen for $q > 1$.

lar behavior as it can be seen in Fig. 4. Again the exponent $\sigma_r(q)$ of the BTW model is characterized by a finite curvature.

The σ exponents of the radius and area distribution are plotted for both models in Fig. 5. In the case of the BTW model the area and radius distributions display in contrast to the size and duration distribution the usual behavior. The q dependence of the exponents $\sigma_a(q)$ and $\sigma_r(q)$ is given by a linear function and the slopes correspond to the trivial values $\gamma_{ar}=2$ (compact avalanches) and $\gamma_{rr}=1$ (see Table I). These exponents are the same for the Manna model and the corresponding curves are parallel. But as Fig. 5 shows there is a clear shift between the curves of the BTW and Manna model, i.e., both models are characterized by two different

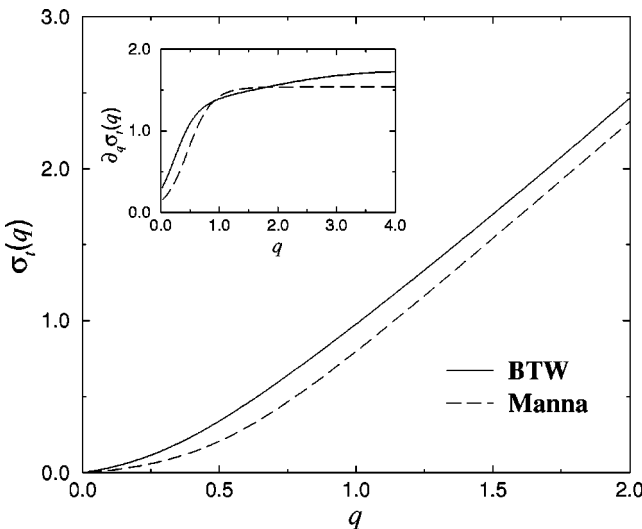


FIG. 4. The exponent $\sigma_r(q)$ of the two-dimensional BTW and Manna model. The derivative of both curves is plotted in the inset and reveals that the exponent $\sigma_r(q)$ of the BTW model displays the same complicated behavior as the exponent $\sigma_s(q)$.

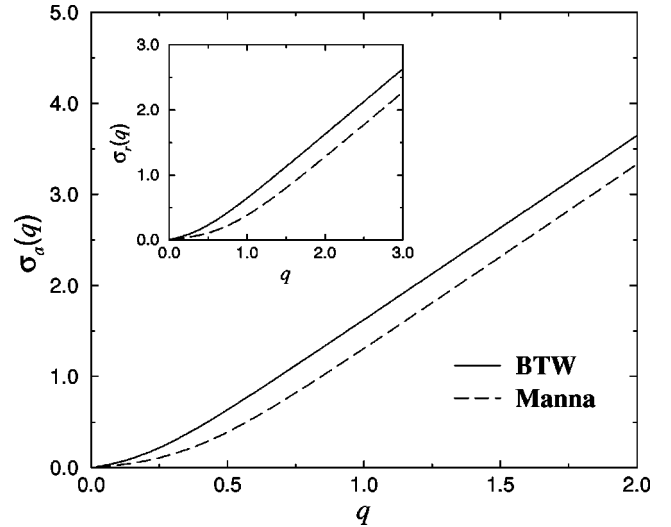


FIG. 5. The exponent $\sigma_a(q)$ and $\sigma_r(q)$ (inset) of the two-dimensional BTW and Manna model. One obtains for both models the same asymptotic slopes (see Table I) which agree with $\gamma_{ar}=2$ and $\gamma_{rr}=1$. But the extrapolation to the horizontal axis yields different values for the models indicating that the BTW and the Manna model are characterized by different avalanche exponents τ_a and τ_r , respectively.

avalanche exponents τ_a and τ_r .

The analysis of the perimeter distribution yields again a simple linear q dependence of the exponents $\sigma_p(q)$ (not shown) and we obtain $\gamma_{pr}=1.266 \pm 0.019$ which corresponds to the fractal dimension of the boundary. This value is in agreement with that obtained from a direct analysis of the scaling relation $p \sim r^{\gamma_{pr}}$ and differs significantly from the value of the Manna model $\gamma_{pr}=1.42$ [8].

Due to the nonlinear behavior of the size and duration distribution we use the area, radius, and perimeter distributions in order to estimate the intercept Σ of the BTW model and obtain $\Sigma_{\text{BTW},2\text{D}}=0.391 \pm 0.011$. But one has to be carefully to compare this result with the corresponding value of the Manna model. The performed moment analysis based on the assumption that the scaling behavior of the BTW model is given by a pure power-law behavior [Eq. (4)]. But this assumption is in contradiction to the observed logarithmic finite-size corrections [4,9] as well as to recently reported investigations where a multifractal behavior of the distribution was observed [11]. In the latter case no avalanche exponent could be defined whereas the analysis of the logarithmic finite-size corrections yield $\Sigma_{\text{BTW},2\text{D}} \approx 2/3$ [9] which again differs significantly from the corresponding value of the Manna model.

These results lead us to the conclusion that the moment analysis is applicable in order to determine the geometric properties of the avalanches of the BTW model, e.g. γ_{ar} , γ_{pr} . The obtained results are in agreement with those of previous investigations which based on different methods of analyzing. But in contrast to the geometric properties the moment analysis of the dynamical properties (size and duration) of the avalanches exhibit a non-trivial behavior. This shows that the assumed simple power-law behavior is not fulfilled and that scaling corrections to Eq. (4) cannot be neglected in these cases. The question whether these corrections can be interpreted in terms of unconventional finite-size

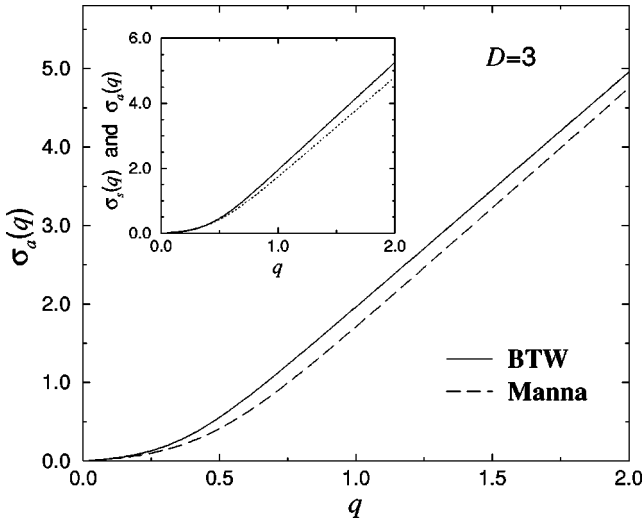


FIG. 6. The exponent $\sigma_a(q)$ of the three-dimensional BTW and Manna model. One obtains for both models the same asymptotic slopes (see Table I) which agree with $\gamma_{ar}=3$ (compact avalanches). In the case of the BTW model both exponents $\sigma_s(q)$ and $\sigma_a(q)$ are plotted, but no difference between the curves can be seen. The inset shows the exponents $\sigma_s(q)$ (solid line) and $\sigma_a(q)$ (dotted line) for the Manna model. The different slopes indicate that multiple toppling events are relevant in the case of the Manna model ($\gamma_{sa} = \gamma_{sr}/\gamma_{ar} > 1$).

effects [4,9], or correspond to a crossover effect from the boundary to the bulk regime [7,10], or indicate a multifractal behavior of the two-dimensional model [11], remains open.

In the following we briefly compare the three-dimensional BTW and Manna model and focus our attention on the analysis of the size and area probability distribution. In Fig. 6 we plot the moment exponent $\sigma_a(q)$ for both models. The result is similar to the two-dimensional case (Fig. 5). The slopes of the curves agree with the value $\gamma_{ar}=3$ indicating that both models are characterized by compact avalanches (see Table I). But the two curves are shifted which shows that the avalanche exponents τ_a of the BTW ($\tau_a=1.352$

± 0.022) and Manna ($\tau_a=1.436 \pm 0.018$) model are different for $D=3$.

The determination of the intercepts Σ confirms this result. Analyzing for both models the size, area, duration and radius distribution we obtain $\Sigma_{\text{BTW},3D}=1.016 \pm 0.056$ and $\Sigma_{\text{Manna},3D}=1.333 \pm 0.036$. The intercepts differs significantly.

Finally we consider the area and size distribution for both models. As mentioned above the three-dimensional Manna model behaves different than the BTW model in the sense that multiple toppling events affects the scaling behavior decisively. This result can also be obtained from the moment analysis. In the case of the BTW model no significant difference between the exponents $\sigma_a(q)$ and $\sigma_s(q)$ can be observed (see Fig. 6). Whereas for the Manna model both curves are characterized by different slopes as can be seen in the inset of Fig. 6. A regression analysis yield $\gamma_{sr}=3.302 \pm 0.06$ and $\gamma_{ar}=3.076 \pm 0.09$, respectively. Thus multiple toppling events affect the scaling behavior of the Manna model strongly ($\tau_s \neq \tau_a$), in contrast to the BTW model.

IV. SUMMARY

In summary we performed a moment analysis of several probability distributions of the BTW and Manna model for $D=2$ and $D=3$. We found that the corresponding moment exponents $\sigma_x(q)$ differ significantly for both models showing that the BTW and Manna model belong to different universality classes. Recently performed simulations of sandpile models on a Sierpinski gasket again the different scaling behavior of both models [31,32]. Our results confirm the universality hypothesis of Ben-Hur and Biham where the scaling behavior of sandpile models is determined by the way in which the relaxing energy of critical sites is distributed to the neighboring sites [8].

ACKNOWLEDGMENT

I would like to thank D. V. Kvitarev for useful discussions and a critical reading of the manuscript.

-
- [1] P. Bak, C. Tang, and K. Wiesenfeld, Phys. Rev. Lett. **59**, 381 (1987).
 - [2] P. Bak, C. Tang, and K. Wiesenfeld, Phys. Rev. A **38**, 364 (1988).
 - [3] D. Dhar, Phys. Rev. Lett. **64**, 1613 (1990).
 - [4] S. S. Manna, J. Stat. Phys. **59**, 509 (1990).
 - [5] P. Grassberger and S. S. Manna, J. Phys. (France) **51**, 1077 (1990).
 - [6] K. Christensen and Z. Olami, Phys. Rev. E **48**, 3361 (1993).
 - [7] P. A. Robinson, Phys. Rev. E **49**, 3919 (1994).
 - [8] A. Ben-Hur and O. Biham, Phys. Rev. E **53**, R1317 (1996).
 - [9] S. Lübeck and K. D. Usadel, Phys. Rev. E **55**, 4095 (1997).
 - [10] S. D. Edney, P. A. Robinson, and D. Chisholm, Phys. Rev. E **58**, 5395 (1998).
 - [11] M. De Menech, A. L. Stella, and C. Tebaldi, Phys. Rev. E **58**, 2677 (1998).
 - [12] A. Chessa, H. E. Stanley, A. Vespignani, and S. Zapperi, Phys. Rev. E **59**, 12 (1999).
 - [13] A. Vázquez and O. Sotolongo-Costa, e-print cond-mat/9811414, 1999 (unpublished).
 - [14] A. Chessa, A. Vespignani, and S. Zapperi, e-print cond-mat/9811365, 1998 (unpublished).
 - [15] S. S. Manna, J. Phys. A **24**, L363 (1991).
 - [16] D. Dhar, Physica A **270**, 69 (1999).
 - [17] D. Dhar and R. Ramaswamy, Phys. Rev. Lett. **63**, 1659 (1989).
 - [18] B. Tadić *et al.*, Phys. Rev. A **45**, 8536 (1992).
 - [19] S. Lübeck, B. Tadić, and K. D. Usadel, Phys. Rev. E **53**, 2182 (1996).
 - [20] B. Tadić and R. Ramaswamy, Physica A **224**, 188 (1996).
 - [21] B. Tadić and D. Dhar, Phys. Rev. Lett. **79**, 1519 (1997).
 - [22] L. Pietronero, A. Vespignani, and S. Zapperi, Phys. Rev. Lett. **72**, 1690 (1994).
 - [23] A. Vespignani, S. Zapperi, and L. Pietronero, Phys. Rev. E **51**, 1711 (1995).
 - [24] M. Katori and H. Kobayashi, Physica A **229**, 461 (1996).

- [25] Y.-C. Zhang, Phys. Rev. Lett. **63**, 470 (1989).
- [26] A. Díaz-Guilera, Europhys. Lett. **26**, 177 (1994).
- [27] Á Corral and A. Díaz-Guilera, Phys. Rev. E **55**, 2434 (1997).
- [28] S. Lübeck, Phys. Rev. E **56**, 1590 (1997).
- [29] A. Díaz-Guilera, Fractals **1**, 963 (1993).
- [30] S. Lübeck and K. D. Usadel, Phys. Rev. E **56**, 5138 (1997).
- [31] F. Daerden and C. Vanderzande, Physica A **256**, 533 (1998).
- [32] F. Daerden and C. Vanderzande (unpublished).